



Using five long time series hydrometeorological data to calibrate a dynamic sediment delivery ratio algorithm for multi-scale sediment yield predictions

Lei Wu^{1,2,3,5,6} · Yin He⁴ · Xiaoyi Ma^{1,6}

Received: 22 November 2019 / Accepted: 14 February 2020 / Published online: 2 March 2020
© Springer-Verlag GmbH Germany, part of Springer Nature 2020

Abstract

The sediment delivery ratio (SDR) is a key link between slope erosion and river sediment transport but the accurate quantification of sediment yield in different catchments has been hampered by a lack of dynamic multi-scale information on SDR. A dynamic multi-scale SDR algorithm was innovatively applied in the modified sediment yield model to quantify the spatiotemporal evolutions of sediment delivery and inventory the relationships between sediment yield and different hydrometeorological and landscape factors in the loess hilly and gully catchment. Results indicate that (i) The sloping farmland (dry lands in hilly areas) in the upstream catchment of Ansai hydrological station was an important sediment source because its soil erosion grade was between intensive and extremely intensive. The high-risk regions of sediment yield were primarily concentrated in the sloping farmlands locating at both sides of the river banks. (ii) The large-scale soil conservation practices since the late 1990s have played a very significant role in sediment reduction. The annual sediment yield rate showed an overall decreasing trend from 1981 to 2015, particularly, it decreased dramatically from $11,844.08 \text{ t}\cdot\text{km}^{-2}$ in 2005 to $65 \text{ t}\cdot\text{km}^{-2}$ in 2015. (iii) The correlations between SDR and sediment yield rate, maximum peak flow, or runoff amount were all greater than that of rainfall parameters, indicating that there was no direct causal relationship between SDR and rainfall indicators in loessial ecological restoration watersheds. Results provide scientific insights needed to guide model modifications and sustainable soil conservation planning in the Loess Plateau.

Keywords Sediment delivery ratio · Dynamic multi-scale algorithm · Sediment yield prediction · Hydrometeorological and landscape factors · Loess hilly and gully region

Introduction

Sediment yield is defined as the amount of eroded soil that is transported by water to a certain point in a landscape or a river system (Lu et al. 2005). Sediment yield at a point along the

main channel of a drainage basin is an integrated result of upland, gully, channel erosion, transportation, and deposition processes (Sen 2014). The sediment delivery ratio (SDR), an important parameter reflecting the sediment yield from an area divided by the gross erosion of the same area (Dong et al.

Responsible Editor: Marcus Schulz

✉ Xiaoyi Ma
xma@nwsuaf.edu.cn

Lei Wu
lwu@nwsuaf.edu.cn

¹ Key Laboratory of Agricultural Soil and Water Engineering in Arid and Semiarid Areas, Ministry of Education, Northwest A&F University, Yangling 712100, Shaanxi, People's Republic of China

² Department of Civil and Environmental Engineering, University of California, Berkeley, Berkeley, CA 94720, USA

³ Blackland Research and Extension Center, Texas A&M AgriLife Research, Texas A&M University, Temple, TX 76702, USA

⁴ Shaanxi Meteorological Information Center, Xi'an 710014, Shaanxi, People's Republic of China

⁵ State Key Laboratory of Soil Erosion and Dryland Farming on the Loess Plateau, Northwest A&F University, Yangling 712100, Shaanxi, People's Republic of China

⁶ College of Water Resources and Architectural Engineering, Northwest A&F University, Yangling 712100, Shaanxi, People's Republic of China

2013), shows a very strong spatiotemporal variability due to the changes of climate, hydrology, topography, soil, land use, and management practices in different regions (Golosov et al. 2017). The main factors influencing SDR can be summarized as three aspects: (i) the landscape and environmental factors, such as drainage area, watershed shapes and channel characteristics (Tang et al. 2001); (ii) the underlying surfaces, such as the size of soil particles, soil texture, vegetation, and land-use types (Cai and Fan 2004); and (iii) the hydrometeorological factors, such as rainfall amount, rainfall duration, runoff depth, runoff coefficient, peak runoff, channel density, gully density, and sediment concentration (Kiniry et al. 2000; Liu et al. 2007).

In general, the SDR algorithms can be classified into four categories (Wu et al. 2018a): (i) the definition of SDR (Zhang et al. 2014); (ii) the single-factor linear, logarithmic, power or polynomial equations based on the watershed area, slope length, river channel slope ratio, runoff, and the valley shape (Zhu et al. 2007; Wu et al. 2020); (iii) the double-factor linear, logarithmic, exponential, or polynomial equations based on the different combination of watershed shape parameters (length, height, width), drainage density, drainage area, runoff, slope, soil infiltration rate, soil erosivity factor, soil particle composition, runoff depth, and rainfall intensity (Wang et al. 2008a); (iv) the multi-factor linear, power or polynomial equations based on the watershed area, elevation, slope, rainfall, curve number (CN), the ratio of height to width, runoff coefficient, rainfall intensity, rainfall duration, antecedent precipitation, the fractal dimension of sediment transport, suspended sediment, gully density, rainfall amount, flood-peak discharge, soil erodibility factor, actual evapotranspiration, potential evapotranspiration, vegetation interception rate, and field water capacity (Wang et al. 2013).

Most of the above SDR algorithms are available and generated by the statistical regression of a large number of experimental or field monitoring data (Xie and Li 2012; Zhang et al. 2014), each with particular strengths and limitations. However, these estimates are largely focused on the long-term average or event-based level of SDR, and the parameters used by the SDR empirical equations are difficult to be obtained in some specific regions, which further limit their practical application scopes (Li et al. 2009a; Gao 2012).

What's more, modeling techniques play a crucial role in the quantitative estimation of soil loss in highly erodible regions (Markose and Jayappa 2016), but there are few dynamic multi-scale studies in the application of SDR because of the obvious difference in the hydrometeorological characteristics of the specific catchments (Wang et al. 2013; Wu et al. 2014); it is usually difficult to establish the most appropriate sediment yield model for the loess hill and gully region (Liu et al. 2007), let alone a universal ensemble modeling approach for multiple scales under long time series hydrometeorological data (Wang et al. 2013). Therefore, there is a tremendous demand to

develop a dynamic multi-scale SDR algorithm which can provide the desired information, be easy to practice, use readily available long-term input data, and instill user confidence and comfort to meet the demands of accurate sediment yield predictions in different catchments.

The aims of this study are to (i) develop a dynamic multi-scale SDR algorithm using five long time series hydrometeorological data of different hydrological stations in the Yanhe River Watershed; (ii) calibrate and evaluate the nonlinear SDR algorithm in multi-scale catchments of the Yanhe River Watershed; and (iii) apply the dynamic SDR algorithm and the modified USLE/RUSLE (Revised Universal Soil Loss Equation) model to predict the spatiotemporal sediment yields in the upstream catchment of Ansai hydrological station.

Materials and methodology

Study region

Yanhe River, with a length of 286.9 km, is the first-grade tributary of the Yellow River, it is originated from Baiyu Mountain and flows through Zhidan, Ansai, Yan'an, and Yanchang counties (cities), and eventually merges into the Yellow River via the Nanhegou River in Yanchang County (Zhang et al. 2005). The Yanhe River Watershed (108° 38' ~110° 29' E and 36° 21'~37° 19' N), with a drainage area of 7725 km², has features of broken and complicated terrain, criss-cross ravines and gullies, and low vegetation coverage. The hilly and gully region accounts for 94.6% of the whole watershed, the gully density is (2.1~4.6) km•km⁻², and the average slope ratio of the river channel is 3.26‰ (Wang et al. 2008b).

The annual average precipitation is 495.6 mm, the annual average runoff is 293 million m³, and the average sediment concentration is 244–311 kg•m⁻³ (Miao et al. 2018). About 75% of annual precipitation, >99.95% of annual runoff, and >94% of annual sediment yield are all concentrated in June–September (Ma et al. 2008). Land-use types in this watershed mainly include forestland, farmland, and grassland. The soil types are dominated by the loessial soil, accounting for >85% of the total drainage area (Zhang et al. 2017). The loessial soil particles are mainly composed of silty sands, which have loose soil structure and poor erosion resistance (Wang and Feng 2017).

There are three important nested hydrological stations in the Yanhe River Watershed, including Ansai, Yan'an, and Ganguyi (Fig. 1). According to geospatial statistics, there are strong geomorphological similarities and small attribute differences in soil, land use, and slope among the three nested catchments, although they differ greatly in the area of catchments. Firstly, the soil types of Calcaric Cambisols and Calcaric Fluvisols (Harmonized World

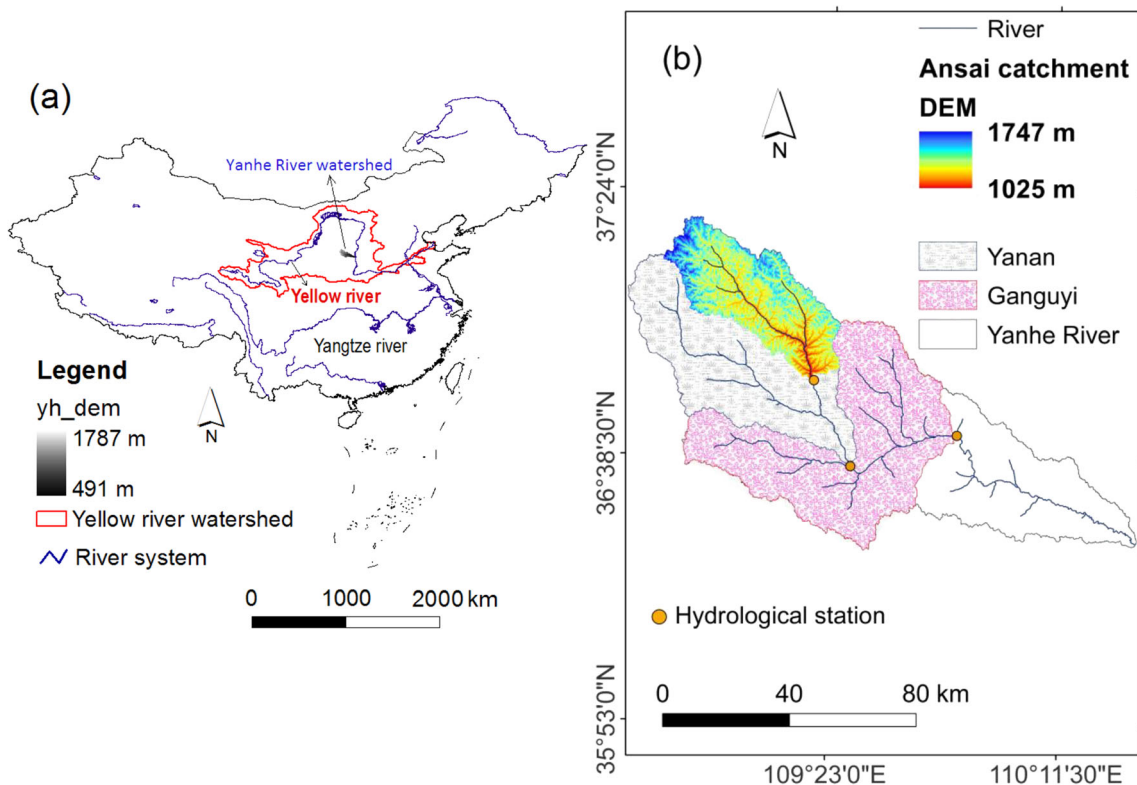


Fig. 1 Study region. **a** The relative location of Yanhe River Watershed in China. **b** Three main catchments in the Yanhe River Watershed: the upstream catchment of Ansaï hydrological station (1334 km²), the

upstream catchment of Yan'an hydrological station (3208 km²), and the upstream catchment of Ganguyi hydrological station (5891 km²)

Soil Database, version 1.1) account for >90% in each catchment, of which the Calcaric Cambisols accounts for >81%. Specifically, the Calcaric Cambisols and Calcaric Fluvisols account for 81.6% and 12.01% in Ansaï catchment, 84.2% and 10.23% in Yan'an catchment, and 81.28% and 9.59% in Ganguyi catchment, respectively. Secondly, the dry land, grassland and forestland are the three main land-use types in each catchment, all accounting for >95%. Among them, the dry lands respectively account for 35.43%, 38.28%, and 40.70% in Ansaï, Yan'an, and Ganguyi catchments; 22.66%, 23.66%, and 16.81% for the middle-coverage grasslands; 32.06%, 28.19%, and 28.59% for the low-coverage grasslands; 6.48%, 4.37%, and 3.12% for the other forestlands; and 0.43%, 0.3%, and 0.44% for the common forestlands. Thirdly, the three catchments all belong to the typical loess hilly and gully regions, and 5–25° slopes account for an absolute advantage of about 85%. Specifically, 0–5° slopes respectively account for 5.49%, 5.07%, and 4.97% in Ansaï, Yan'an, and Ganguyi catchments; 27.2%, 25.21%, and 25.25% for 5–10° slopes; 35.89%, 35.79%, and 36.51% for 10–15° slopes; 22.73%, 24.71%, and 25.07% for 15–20° slopes; 7.58%, 8.2%, and 7.5% for 20–25° slopes; and 1.11%, 1.01%, and 0.69% for >25° slopes.

The Ansaï hydrological station, one of the three primary hydrological stations in the Yanhe River Watershed, is located in the second sub-regions of Chinese loess hilly and gully region (Fig. 1). The annual average runoff amount is about 48.7 million m³. The upstream catchment of Ansaï hydrological station, with an area of 1334 km², has a steep slope, deep gully, and easily eroded loessial soil. Grassland and sloping farmland (dry land) are the main land-use types that account for about 89.09% of the total catchment area. To reduce soil erosion, a series of soil and water conservation practices such as warp land dams, terracing, contour tillage, eco-clean small watershed, man-made afforestation and grass planting, and the natural recovery of forestland or grassland by land closure were successively implemented in the Loess Plateau since the 1950s (Wu et al. 2020). More significantly, the historically unprecedented project, “Grain-for-Green,” was officially initiated in western China for soil erosion control and vegetation improvement by converting sloping farmland into forests or grassland in 1999 (Wang et al. 2006).

Data sources and descriptions

The environmental database, which includes the digital elevation model (DEM) (Fig. 2), land-use types (Fig. 3),

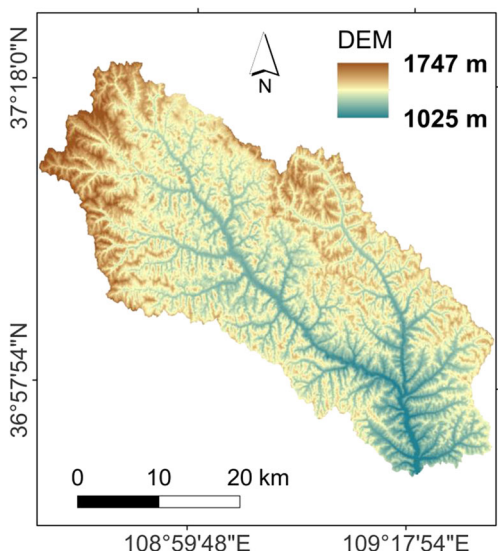


Fig. 2 Digital Elevation Model (DEM) in the upstream catchment of Ansai hydrological station

normalized difference vegetation index (NDVI), soil properties, runoff, sediment, and meteorological data, is given in Table 1.

Dynamic sediment yield model

An important consideration in selecting a model is whether an established user base exists for the model (Toy et al.

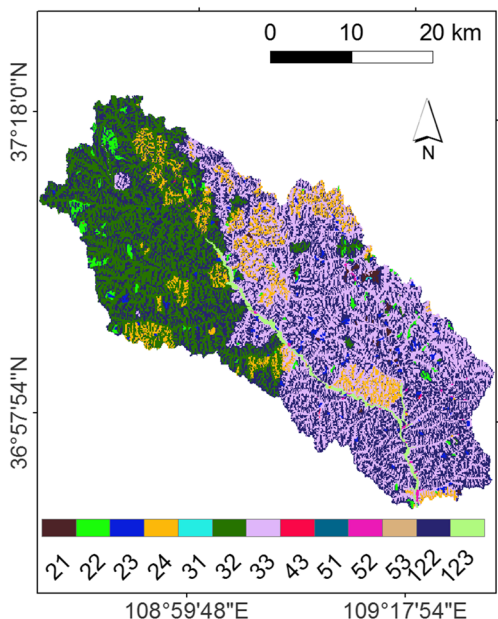


Fig. 3 Spatial distribution of 2010 land-use types in the upstream catchment of Ansai hydrological station (21 forest land, 22 shrubland, 23 sparse forest land, 24 other forest land, 31 high coverage grassland, 32 middle-coverage grassland, 33 low-coverage grassland, 43 reservoir or pond, 51 urban, 52 rural residential area, 53 industrial, traffic, and constructional land, 122 dry land in hilly area, 123 dry land in plain area)

2002). The USLE/RUSLE was selected as the original version to modify the dynamic sediment yield model (Kinnell 2016). This is because the USLE/RUSLE model is now frequently used for erosion estimates at a catchment scale by combining with GIS spatial analysis techniques (de Vente et al. 2008; Mhangara et al. 2012; Akbarzadeh et al. 2016), although it was originally designed for estimating long-term average sheet and rill erosion from specific field slopes in specified cropping and management systems and from rangeland (Wischmeier and Smith 1978; Renard et al. 1997). In the process of studying the dynamic sediment yield model based on geospatial technology, the following three issues need to be emphatically considered: (i) ephemeral gully, one of the main ways of soil erosion in the middle and lower parts of slopes (Jiang et al. 2005), is a typical kind of erosion channel formed due to the alternative action of runoff scouring and tillage in the Loess Plateau of China (Kang et al. 2016); (ii) the topography and soil types in a watershed are basically unchanged for a relatively short time (Long et al. 2012), so the factors of K , L , and S that reflect topographical features and soil properties can be assumed to be constants in the USLE/RUSLE model; and (iii) the hydrometeorological situations and land management practices changed greatly year by year (Wu et al. 2016a; Molla and Sisheber 2017), so the factors of R , C , P , and λ might change at any time with climatic conditions and human activities (Wu et al. 2016b). Thus, the USLE/RUSLE model can be modified as the dynamic sediment yield model:

$$Q_{s,i} = K \cdot L \cdot S \cdot G \cdot R_i \cdot C_i \cdot P_i \cdot \lambda_i \tag{1}$$

where Q_s is the average annual sediment yield rate, $t \cdot km^{-2} \cdot year^{-1}$; K is the soil erodibility factor, $t \cdot ha \cdot h \cdot ha^{-1} \cdot MJ^{-1} \cdot mm^{-1}$; LS is the slope length and slope gradient factor (topographic factor); G is the ephemeral gully erosion factor; R is the rainfall-runoff erosivity factor, $MJ \cdot mm \cdot ha^{-1} \cdot h^{-1} \cdot year^{-1}$; C is the cover and management factor; P is the support practice factor; λ is the average sediment delivery ratio (SDR) factor; subscript i represents the i -th year and no subscript for the average year.

The variation of R_i in Eq. (1) depends only on the meteorological conditions while C_i and P_i only on the land management activities, but λ_i depends not only on hydrometeorological conditions but also on land management activities. Supposing that the factor expression of $C_i \cdot P_i \cdot \lambda_i$ can be approximately defined as the product of $C \cdot P$ and the comprehensive SDR factor (SDR_i), Eq. (1) can be rewritten as:

$$Q_{s,i} = K \cdot L \cdot S \cdot G \cdot R_i \cdot C \cdot P \cdot SDR_i \tag{2}$$

where SDR_i the comprehensive SDR factor that is not only related to hydrometeorological conditions but also to land management activities.

Table 1 Sources and descriptions of the environmental database in the study region

Name	Format	Description	Source
DEM	Raster	30-m resolution Digital Elevation Model (DEM)	Data cloud of Chinese Academy of Sciences (http://www.gscloud.cn/)
Land use	Raster	100-m Landsat TM/ETM remote sensing image (2010)	Geographical Information Monitoring Cloud Platform (http://www.dsac.cn/)
NDVI	Raster	250-m Landsat TM/ETM, MODIS and AVHRR satellite remote sensing image (2000–2015)	
Soil properties	Excel	Soil mechanical composition, organic carbon	Loess Plateau Data Center, National Earth System Science Data Sharing Infrastructure, National Science & Technology Infrastructure of China (http://loess.geodata.cn/)
Runoff and sediment	Excel	Annual runoff, maximum peak flow, sediment transport rate in Ansai, Yan’an, and Ganguyi hydrological stations (1981–2015)	
Meteorological data	DBF	Daily precipitation from weather stations adjacent to or within the catchment (1981–2015)	China Meteorological Data Sharing Service Network (http://data.cma.cn/) Shaanxi Meteorological Bureau http://sn.cma.gov.cn

Factor algorithms

R factor

The rainfall erosivity factor (*R*) was estimated by an approach proposed by Renard and Freimund (1994). This approach is based on an empirical relationship between rainfall erosivity and the Fournier Index (*FI*), and has been applied in various watersheds (Beskow et al. 2009; Diodato and Bellocchi 2010). The specific equations of *R* factor are as follows,

$$FI_{i,j} = \frac{p_{i,j}^2}{p_i} \tag{3}$$

$$r_{i,j} = \frac{125.92 \cdot FI_{i,j}^{0.603} - 111.173 \cdot FI_{i,j}^{0.691} + 68.73 FI_{i,j}^{0.841}}{3} \tag{4}$$

$$R_i = \sum_{j=1}^{12} r_{i,j} \tag{5}$$

where $FI_{i,j}$ is the *FI* for month *j* in the *i*-th year; $p_{i,j}$ is the monthly rainfall (mm) for month *j* in the *i*-th year; p_i is the annual rainfall (mm) in the *i*-th year; and $r_{i,j}$ is the monthly rainfall-runoff erosivity for month *j* in the *i*-th year ($MJ \cdot mm \cdot ha^{-1} \cdot h^{-1} \cdot month^{-1}$). R_i is the annual rainfall-runoff erosivity factor in the *i*-th year ($MJ \cdot mm \cdot ha^{-1} \cdot h^{-1} \cdot year^{-1}$).

K factor

The soil erodibility factor, *K*, is a quantitative value experimentally determined in the USLE/RUSLE model (Alewell et al. 2019). It can be calculated by the following empirical equation (Liu et al. 2010; Zhang et al. 2007),

$$K = \left\{ 0.2 + 0.3 \exp \left[-0.0256 S_a \left(1 - \frac{S_i}{100} \right) \right] \right\} \left(\frac{S_i}{C_i + S_i} \right)^{0.3} \times \left[1 - \frac{0.25 C_0}{C_0 + \exp(3.72 - 2.95 C_0)} \right] \times \left[1 - \frac{0.7 S_n}{S_n + \exp(-5.51 + 22.9 S_n)} \right] \tag{6}$$

where *K* is the soil erodibility factor, $t \cdot ha \cdot h \cdot ha^{-1} \cdot MJ^{-1} \cdot mm^{-1}$; S_a is the sand mass fraction (0.05~2 mm), %; S_i is the silt mass fraction (0.002~0.05 mm), %; C_i is the clay mass fraction (< 0.002 mm), %; and, C_0 is the percentage of organic matter, %.

LS factor

The topographical factor (*LS*) is an important index to characterize the effect of terrain on soil erosion (Wang et al. 2004). Both the slope length and the slope steepness affect the rate of soil erosion substantially (Yavuz and Tufekcioglu 2019). The two factors have been evaluated and represented in the USLE/RUSLE model by *L* and *S* respectively (Wischmeier and Smith 1978).

The *L* factor values were estimated by the formulas proposed by Wischmeier and Smith (1965) and Foster and Wischmeier (1974). The specific equations based on the location of DEM grid are as follows,

$$L_i = \frac{\lambda_{out}^{m+1} - \lambda_{in}^{m+1}}{(\lambda_{out} - \lambda_{in})(22.13)^m} \quad \lambda_{out} - \lambda_{in} > 0 \tag{7}$$

$$L_i = \left(\frac{\lambda_{out}}{22.13} \right)^m \quad \lambda_{out} - \lambda_{in} < 0 \tag{8}$$

$$L_i = L_{flow} \quad \lambda_{out} - \lambda_{in} = 0 \tag{9}$$

$$L_i = 0 \quad \lambda_{out} = 0 \tag{10}$$

where L_i is the slope length factor in the *i*-th grid, L_{flow} is defined as the slope length factor in the grid with the longest flow path, λ_{out} and λ_{in} are the slope length respectively in the grid outlet and the grid inlet, *m* is the slope length index.

The slope length index can be determined by the previous research results (Liu et al. 2000),

$$\begin{aligned}
 m = 0.2 & \quad \theta < 0.5^\circ \\
 m = 0.3 & \quad 0.5^\circ \leq \theta < 1.5^\circ \\
 m = 0.4 & \quad 1.5^\circ \leq \theta < 3^\circ \\
 m = 0.5 & \quad 3^\circ \leq \theta
 \end{aligned} \quad (11)$$

where θ is the slope gradient ($^\circ$).

The S factor values in the gentle slope ($\leq 10^\circ$) and steep slope ($> 10^\circ$) were respectively calculated by the formulas proposed by McCool et al. (1987) and Liu et al. (2010). The specific piecewise expressions are as follows,

$$\begin{aligned}
 S &= 10.8\sin\theta + 0.03 & \theta < 5^\circ \\
 S &= 16.8\sin\theta - 0.5 & 5^\circ \leq \theta \leq 10^\circ \\
 S &= 21.9\sin\theta - 0.96 & \theta > 10^\circ
 \end{aligned} \quad (12)$$

where S is the slope gradient factor, θ is the slope gradient ($^\circ$).

C factor

The cover and management factor (C) is the ratio of soil loss from an area with specified cover and management to that from an identical area in tilled continuous fallow (Wischmeier and Smith 1978). The C factor can be estimated by the equations proposed by Cai et al. (2000) and Ma et al. (2001). The specific expressions are as follows,

$$c_j = \frac{NDVI_j - NDVI_{soil,j}}{NDVI_{veg,j} - NDVI_{soil,j}} \quad (13)$$

$$C_j = \begin{cases} 1 & c_j = 0 \\ 0.6508 - 0.3436 \lg c_j & 0 < c_j < 78.3\% \\ 0 & c_j \geq 78.3\% \end{cases} \quad (14)$$

$$C = \sum_{j=1}^{12} \frac{R_j}{R} C_j \quad (15)$$

where c_j is the monthly vegetation coverage (%), $NDVI_{soil,j}$ is the Normalized Difference Vegetation Index (NDVI) value of nonvegetated areas (or, NDVI of a pure soil pixel), $NDVI_{veg,j}$ is the NDVI value of vegetated areas (or, NDVI of a pure vegetation pixel). C_j is the monthly cover and management factor, C is the annual cover and management factor, R_j is the monthly rainfall-runoff erosivity factor, R is the annual rainfall-runoff erosivity factor.

P factor

The support practice factor (P) in the USLE/RUSLE model is the ratio of soil loss with a specific support practice to the corresponding soil loss with up-and down-slope cultivation (Wischmeier and Smith 1978). The most important cropland supporting practices are contour tillage, strip cropping, and terraces. The P factor values were determined by different support practices under different land-use types (Cheng et al. 2012; Xie 2008).

G factor

The ephemeral gully erosion factor (G) reflects the effects of the shallow gully on the processes of soil erosion (Zheng and Xiao 2010). G factor was primarily affected by precipitation, the convergent intensity of flow, slope steepness, slope length, and soil properties (Jiang et al. 2008). According to the previous studies (Li et al. 2009b; Wu et al. 2016c), the specific equation was determined as follows:

$$G = 1 + \sigma = 1 + \frac{(\alpha - \theta_c) \left(1.003(R_e \cdot I_{30})^{0.013} - 1 \right)}{30 - \theta_c} \quad (16)$$

where: G is the ephemeral gully erosion factor; σ is the correction coefficient; α is the surface slope ($^\circ$); θ_c is the critical slope gradient ($^\circ$); R_e is the event-based rainfall amount (mm); I_{30} is the 30-min maximum rainfall intensity (mm/min); when there is no ephemeral gully erosion on the slope, $\sigma = 0$, and $G = 1$; when the slope gradient is $< 15^\circ$, $G = 1$.

SDR factor

The rainfall, runoff, rainfall erosivity, maximum peak flow, and the sediment transport rate were exactly proven to be the main hydrometeorological factors affecting the sediment yield processes in the loess hilly and gully region (Wu et al. 2018b). Meanwhile, the comprehensive surface roughness factor estimated by the long time series data of soil erosion and sediment yield from 1957 to 1989 was introduced to dynamically identify the potential impacts of the underlying surfaces on sediment transport under different catchment scales. Based on these two prerequisites, the annual SDR values in the upstream catchment of Ansai hydrological station were used to develop and calibrate the dynamic SDR algorithm by the repeated multivariate nonlinear regression, while the statistical sediment transport rate of the large-scale loess hilly catchments was used to fit the equation of the comprehensive surface roughness factor,

$$SDR_i = 9.3644Q_i^{-0.14045} RI_i^{-0.80984} F_i^{-0.053245} S_i^{1.0861} P_i^{-0.19049} N_i \quad (17)$$

$$N_i = 0.5834e^{-0.00009 S_i} \quad (R^2 = 0.58, n = 33, p < 0.05) \quad (18)$$

where SDR_i is the annual SDR value, Q_i is the annual runoff amount (10^4 m^3), RI_i is the annual rainfall intensity ($\text{MJ} \cdot \text{mm} \cdot \text{hm}^{-2} \cdot \text{h}^{-1} \cdot \text{year}^{-1}$), F_i is the annual maximum peak flow ($\text{m}^3 \cdot \text{s}^{-1}$), S_i is the annual average sediment transport rate ($\text{kg} \cdot \text{s}^{-1}$), P_i is the annual rainfall amount (mm), N_i is annual comprehensive land roughness factor ($N_i = 1$, when the watershed area is equal to 1334 km^2).

Factor estimation and rasterization

The mean estimated values of *R*, *K*, *LS*, *CP*, *G* and SDR in the upstream catchment of Ansai hydrological station are given in Table 2.

The *R*, *K*, *LS*, *CP* factors were respectively calculated by rasterization and shown in Fig. 4.

Results

Calibration performance of the SDR algorithm

The measured SDR by its definition from 1981 to 2015 and the calculated SDR by the developed SDR algorithm were compared to test the calibration performance in the upstream catchment of Ansai hydrological station Fig. 5. The specific results are as follows: (i) The SDR values calculated by the dynamic algorithm were close to the SDR values by the definition method ($y = 1.0006x - 0.0114$, $R^2 = 0.986$, $n = 35$, $p < 0.01$), the relative error ranges between -24.3% and 10.91%, which confirms that the dynamic SDR algorithm had good applicability in the upstream catchment of Ansai hydrological station. (ii) Although the SDR values in individual years were relatively large, the calculated SDR in the upstream catchment of Ansai hydrological station presented an overall decreasing trend, and this trend was well consistent with the effective implementation of the large-scale “Grain for Green” project in Western China since 1997, which also indicates that the dynamic SDR algorithm had strong applicability in the ecological restoration regions. Moreover, the sharp decrease of SDR after 2005 supported again that the reduction benefits of runoff and sediment by soil conservation practices were considerable. (iii) The variation trends of SDR from 1981 to 2015 were highly consistent with the sediment yield rate ($y = 0.0001x + 0.036$, $R^2 = 0.834$, $n = 35$, $p < 0.01$), maximum peak flow ($y = 0.0018x + 0.0579$, $R^2 = 0.68$, $n = 35$, $p < 0.05$), and runoff amount ($y = 0.0004x - 1.1095$, $R^2 = 0.658$, $n = 35$, $p < 0.05$), indicating that the linear correlation between SDR and sediment yield rate was more significant than the other two hydrological factors in the upstream catchment of Ansai hydrological station. The relative importance of maximum peak flow and runoff amount in the erosion processes was similar although the impact of maximum peak flow was slightly higher than runoff amount. (iv) The correlations between SDR and

rainfall amount ($y = 1.0095e^{-0.0017x}$, $R^2 = 0.0196$, $n = 35$, $p > 0.05$) or rainfall erosivity ($y = -0.2943\ln x + 2.9727$, $R^2 = 0.029$, $n = 35$, $p > 0.05$) in the upstream catchment of Ansai hydrological station were both very weak, indicating that there was no direct causal relationship between SDR and rainfall indicators in the loess hilly and gully regions. In other words, soil erosion (soil detachment) is not equal to sediment yield, the eroded soil was not always able to be delivered from the eroding portions of a hillslope to the outlet of a watershed (sediment yield) before deposition due to the effective runoff and sediment reduction effects of large-scale soil conservation practices (Wu et al. 2020), although the heavy rainstorms might cause serious soil erosion. (v) There were still high sediment yield rates in 2004 and 2005 although the SDR values in these 2 years decreased significantly due to the effective implementation of soil conservation practices since 1997, indicating that the SDR dynamics might be more sensitive and identifiable to the soil conservation practices than the sediment yield rate.

Spatial variations of sediment yield

The spatial distributions of soil erosion grade and sediment yield rate varied greatly in the upstream catchment of Ansai hydrological station in 2010 (Fig. 6). The soil erosion grade ranged from micro erosion to severe erosion, and the percentages of micro, mild, moderate, intensive, extreme, and severe erosion accounted for 2.35%, 0.31%, 11.51%, 39.73%, 27.12%, and 18.99% respectively, which indicates that the proportion of high erosion rates (> intensive) was particularly evident in the upstream catchment of Ansai hydrological station in 2010 with a total sum of 85.84%. The extreme erosion and severe erosion were mostly located in the northwest mountainous regions, in reverse, the micro erosion and mild erosions were located in the southeast of the catchment, but there were also some scattered extreme erosion zones in the middle and lower reaches of the catchment. The above results are related not only to the spatial distribution of erosive rainstorms in 2010 but also to the implementation background and effect of the large-scale soil conservation practices since 1997.

Unlike soil erosion grade, the sediment yield rate in the middle and lower reaches of Ansai hydrological station was still severe particularly in the case of heavy rainstorms and intense human activities in 2010, although the large-scale soil conservation practices had been effectively implemented since 1997. The sediment yield risk map also suggests that the regions with

Table 2 Mean value of each factor in the modified sediment yield model

Factor	<i>R</i> (MJ•mm•ha ⁻¹ •h ⁻¹ •year ⁻¹)	<i>K</i> (t•ha•h•ha ⁻¹ •MJ ⁻¹ •mm ⁻¹)	<i>LS</i>	<i>CP</i>	<i>G</i>	SDR (1981–2015)
Mean	1762.92	0.01765	12.9	0.0835	1.327	0.81

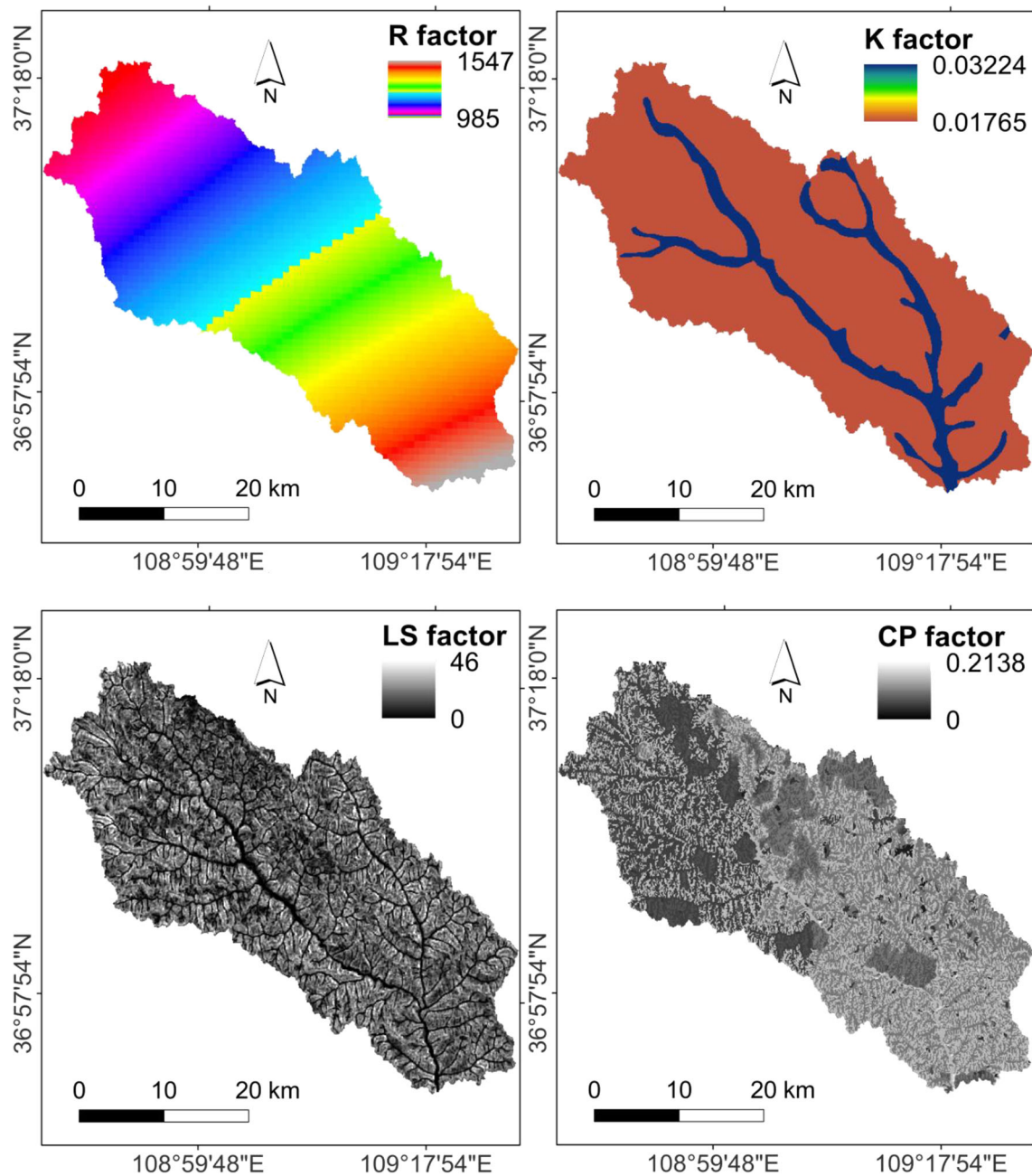


Fig. 4 Spatial distribution of the rainfall-runoff erosivity factor (R) ($\text{MJ}\cdot\text{mm}\cdot\text{ha}^{-1}\cdot\text{h}^{-1}\cdot\text{year}^{-1}$), the soil erodibility factor (K) ($\text{t}\cdot\text{ha}\cdot\text{h}\cdot\text{ha}^{-1}\cdot\text{MJ}^{-1}\cdot\text{mm}^{-1}$), the topographic factor (LS), the cover and

management factor (C), and the support practice factor (P) in the upstream catchment of Ansai hydrological station in the Yanhe River Watershed

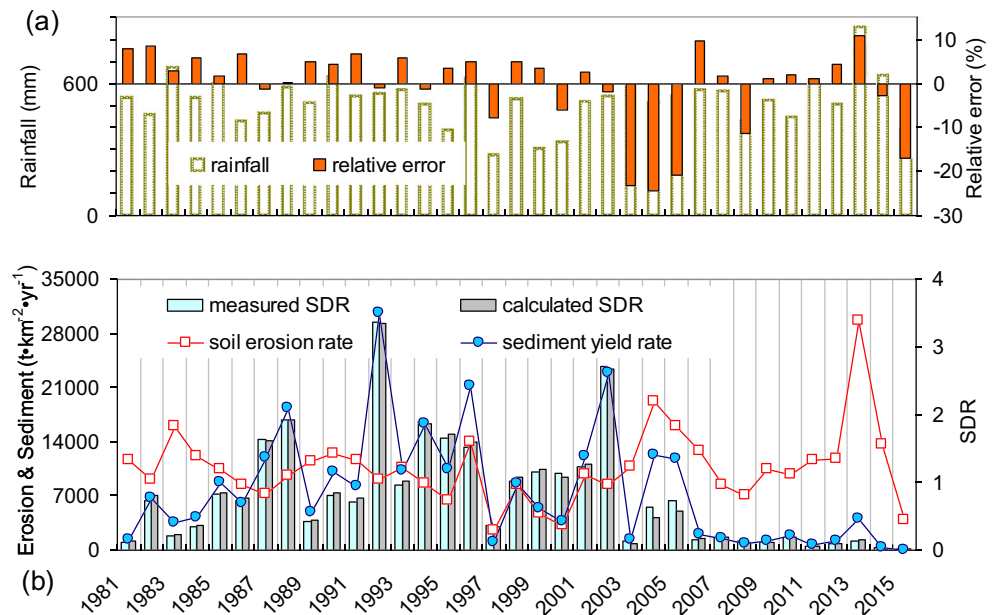
greatest sediment yield potential were primarily concentrated in the extensive sloping farmlands located at the two sides of main river banks from northwest to southeast of the catchment, but the peak sediment yield rate gradually decreased as the distance from the river bank increased.

Temporal variations of sediment yield

The temporal variations of sediment yield rate, rainfall erosivity and runoff amount in the upstream catchment of Ansai

hydrological station are presented in Fig. 5b. First, the sediment yield rate showed an overall decreasing trend from 1981 to 2015. The maximum sediment yield rate in the upstream catchment of Ansai hydrological station appeared in 1992 with a value of $30,700 \text{ t}\cdot\text{km}^{-2}$, while the minimum occurred in 2015 with a value of $65 \text{ t}\cdot\text{km}^{-2}$. Second, the average annual sediment yield rate from 1981 to 1997 was $10,238.35 \text{ t}\cdot\text{km}^{-2}$, there was no obvious downward trend for annual sediment yield rate during this period, on the contrary, a sharp increase of the sediment yield rate occurred in 1992. Third, after 1997,

Fig. 5 Calibration results of the dynamic sediment delivery ratio (SDR) algorithm in the upstream catchment of Ansai hydrological station from 1981 to 2015. **a** Rainfall (mm) and relative error between measured SDR and calculated SDR (%). **b** Trends of soil erosion rate ($t \cdot km^{-2} \cdot year^{-1}$), sediment yield rate ($t \cdot km^{-2} \cdot year^{-1}$), measured SDR, and calculated SDR



the annual sediment yield rate presented a very significant downward trend, and particularly, the annual sediment yield rate decreased dramatically from $11,844.08 t \cdot km^{-2}$ in 2005 to $65 t \cdot km^{-2}$ in 2015.

The sediment yield rate presented a significantly positive correlation with runoff amount ($y = 3.7509x - 10,664$, $R^2 = 0.730$, $n = 35$, $p < 0.05$), although there were several conspicuous mutation points in the trend line of sediment yield rate and runoff amount from 1981 to 2015, e.g., the

annual sediment yield rates in 1988, 1992, 1996 and 2002 were $18,300$, $30,700$, $21,200$, and $22,900 t \cdot km^{-2}$, respectively, which are significantly higher than the average level. However, the interactions between sediment yield rate and rainfall erosivity were relatively complex in the upstream catchment of Ansai hydrological station, and there was no obvious correlation between sediment yield rate and rainfall erosivity ($y = 2628.8e^{0.0003x}$, $R^2 = 0.024$, $n = 35$, $p > 0.05$).

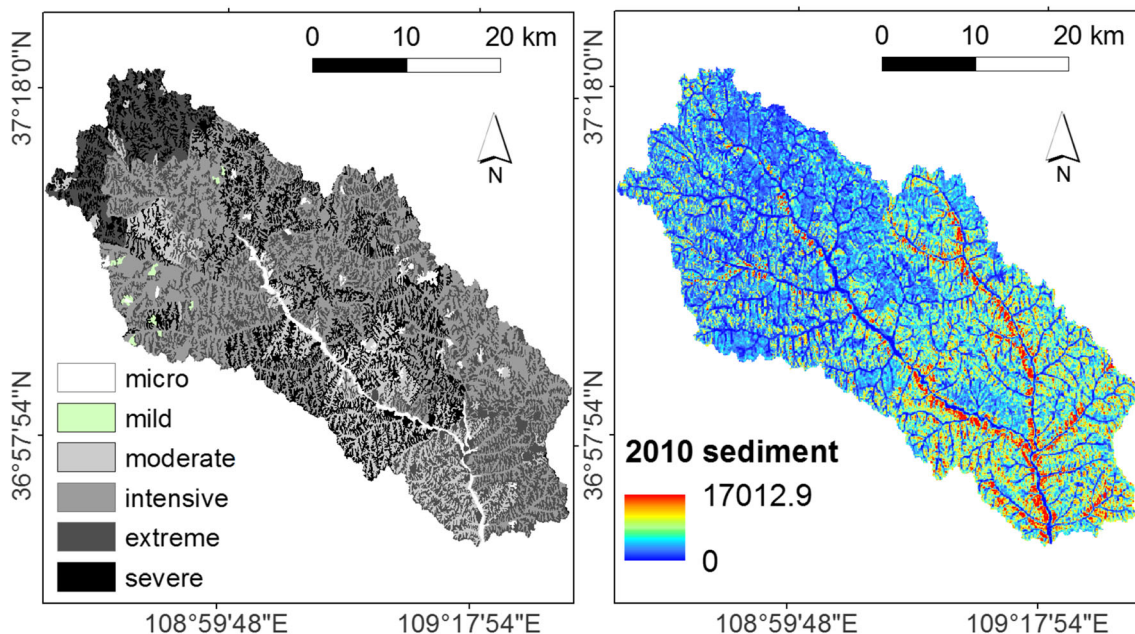


Fig. 6 Spatial distribution of soil erosion grade and sediment yield rate ($t \cdot km^{-2}$) in the upstream catchment of Ansai hydrological station in 2010. Chinese Soil Erosion Classification and Grading Standards (SL190–2007): water erosion (a) micro (< 200 , < 500 , $< 1000 t \cdot km^{-2} \cdot year^{-1}$),

(b) mild (200 , 500 , 1000 – $2500 t \cdot km^{-2} \cdot year^{-1}$), (c) moderate (2500 – $5000 t \cdot km^{-2} \cdot year^{-1}$), (d) intensive (5000 – $8000 t \cdot km^{-2} \cdot year^{-1}$), (e) extremely intensive (8000 – $15,000 t \cdot km^{-2} \cdot year^{-1}$), and (f) severe ($> 15,000 t \cdot km^{-2} \cdot year^{-1}$)

Discussion

Evaluation of the dynamic multi-scale SDR algorithm

The average observed sediment yield rates in different catchment scales were used to verify the confidence and reliability of the modified sediment yield model (Table 3). The main findings might involve the following: (i) The average relative errors between the simulated and observed sediment yield rates in the upstream catchments of Ganguyi (1952–2013), Yan'an (1958–2007) and Ansai (1981–2015) hydrological stations were -11.7% , 6.2% , and 10.7% respectively. These acceptable relative errors illustrate that the combination of the dynamic multi-scale SDR algorithm and the modified USLE/RUSLE model was reliable and feasible for the improvement of prediction accuracy of sediment yield, and it could be used as a powerful methodology tool in evaluating the dynamic evolutions of sediment yield in any other ecological restoration regions. (ii) The introduction of G factor in the modified sediment yield model has been proven to be important for improving the estimation accuracy of soil erosion in the loess hilly and gully region. This is because the soil erosion caused by ephemeral gullies contributes greatly to the total soil losses and is one of the major processes of land degradation (Taguas et al. 2012), moreover, the gullies in cultivated fields are not only the main channel of sediment transport (Martinez-Casasnovas et al. 2005) but also the main source of eroded soil particles (Zhu 2012). (iii) Although the SDR values in the dry period were always found to be lower than that in the flood period (Woznicki and Pouyan Nejadhashemi 2013), the dynamic SDR algorithm can be successfully applied in the spatiotemporal sediment yield predictions of the ecological restoration watersheds. More importantly, the structure and function of the sedimentary cascade in a watershed can still provide useful information for the design of cost-effective hydrological surveys and appropriate conservation planning and mitigation strategies (Yu et al. 2011). (iv) This novel approach for modeling sediment input to surface waters has less uncertainty originating from the sporadic model variability (Wang et al. 2013), which can be considered as part of the particulate nutrient loss model for the source-differentiated quantification of dynamic nutrient inputs in large river basins or landscapes (Tetzlaff et al. 2009). (v) The correlation between SDR and sediment yield rate in the upstream catchment of Ansai hydrological station is similar to the findings that the SDR values

were positively related to the sediment yield rate in Chabagou River Watershed (Liu et al. 2007). Overall, the above new understanding may provide key insights into the development of a time-space scale transformation methodology framework of regional sediment yield predictions (Ondráčková and Máčka 2019).

In general, the model selection criteria are primarily based on either model performance or consensus (Lin et al. 2018). Although the modified model shows promising results in modeling the spatiotemporal sediment yield characteristics in multi-scale catchments, it is still far from achieving performance comparable to that of other physically-based watershed models in the microscopic mechanism of the sediment transport process (Keesstra et al. 2014; Batista et al. 2017). In other words, the model still has some limitations that can be improved in the future, e.g., (i) the scale extension of SDR algorithm is only based on the difference of comprehensive roughness coefficient factor, which is likely to be an abstractive, black-box concept that lacks the in-depth interpretation of spatial scale effect for different catchments (Wu et al. 2017), so the future model improvements will focus on the effective integration in dynamic variation and spatial visualization of sediment delivery based on the hydrometeorological and topographical data (Lee and Kang 2013); (ii) the model structure is of utmost importance since it determines both how the real-world phenomena are simplified and whether the complex input data are required (Watling et al. 2015), but the physical mechanism deficiency of the multi-scale SDR algorithm and the complexity of sediment transport process increase the uncertainty of the empirical-based modified model (Tetzlaff et al. 2013), it is essential to continue examining both the sources of model uncertainty and the effects they have on the key source identification and the mitigation practice application (Swarnkar et al. 2018); (iii) the dynamic multi-scale SDR algorithm based on rainfall, runoff, rainfall erosivity, maximum peak flow, sediment transport rate, and underlying surfaces are more sensitive to soil conservation practices, but the model output is at the grid level rather than the hydrological response unit (HRU) level, affecting the identification accuracy of highly eroded areas, so it is often exceedingly difficult or impractical to select the optimal best management practices (BMPs) for all priority control regions considered in a specific conservation initiative (Sarma et al. 2015); (iv) the modified sediment yield model has primarily relied upon annual hydro-meteorological data; however, the widely available data such

Table 3 Comparison of the average simulated and observed sediment yield rates in the three upstream catchments of Ganguyi, Yan'an, and Ansai hydrological stations

Hydrological station	Simulated sediment yield rate ($t \cdot km^{-2} \cdot year^{-1}$)	Observed sediment yield rate ($t \cdot km^{-2} \cdot year^{-1}$)	Relative error (%)
Ganguyi	5958.47	6747.68	-11.7
Yan'an	5448.37	5131.06	6.2
Ansai	6789.32	7603.54	10.7

as event-based or daily precipitation and discharge are disregarded resulting in a reduction in temporal accuracy (Temme et al. 2011); (v) the importance of this modeling tool is practical, but understanding the relationships between patterns at various scales cannot be strictly done with this modeling tool because it has no close connection with physically-based erosion processes and can only prove post-factum effects when the catchments are rather large. Most noteworthy, the existing large data sets might be used in the future process-based erosion models, especially for the multi-scale patterns of sediment production; and, (vi) undeniably, the innovative process-based modeling framework of distributed hydrological model and sediment yield model, by integrating long time series hydrometeorological data, geographical information system (GIS) and remote sensing techniques, and the four modules of raindrops splashing, soil detachment, runoff driven and sediment routing, will become the key direction of soil erosion research at catchment scales (Wu et al. 2019a). It can not only overcome the limitation of the deficiency of physical mechanism of the USLE/RUSLE model but also can estimate the erosion potential and identify critical erosion-prone areas in watersheds effectively, which can eventually provide strategy support for policy-makers and practitioners.

Spatial analysis of soil erosion and sediment yield

The soil erosion grade and sediment yield rate under different land-use types differed greatly in the upstream catchment of Ansai hydrological station in 2010 (Table 4). The land-use types were mainly composed of dry land in hilly area, middle-coverage grassland, and low-coverage grassland, accounting for 35.76%, 22.25%, and 31.08% of the total catchment area respectively. The soil erosion grades of these three land-use types were all between intensive erosion and extreme intensive erosion. The results exactly conform to the dominated grade level of extreme erosion in the second sub-regions of loess hilly and gully region (Wang et al. 2003). The largest sediment yield amount occurred in the hilly dry land area (sloping farmland) with a value of 124.901×10^4 tons. The results are similar to the sediment yield level under different land-use types in purple soil: farmland>orchard>grassland>shrubland>forestland (Zhang and Li 2018). Therefore, it is of great significance to implement effective soil conservation practices in sloping farmland and low-coverage grassland for sustainable agriculture (Wu et al. 2019a). However, the maximum sediment yield rate appeared in the rural residential area, which can be primarily attributed to the relatively large sediment source and small areal size of rural settlements (Ndomba et al. 2009).

Catchment estimates of sediment yield and its spatial and temporal variations are needed for the evaluation of the effects of various land-use management practices (Sadeghi et al. 2008). The high-risk regions of sediment source in the upstream catchment of Ansai hydrological station were mainly

from the hilly dry land, middle-coverage grassland, low-coverage grassland, and other forest lands. This is because soils are generally vulnerable and lands are often degraded with steep slopes and declining vegetation cover (Steege et al. 2001), and the increase of agricultural activities inevitably causes the increase of sediment yield (Huang and Lo 2015). The results are similar to the findings by Op de Hipt et al. (2019) that the enlarging cropland was an important and growing contribution source to total soil loss in a tropical West African catchment. The results also support the fact that hill slopes are the primary source of erosion by pulsed runoff with channel bank and flood plains as the secondary sources in arid regions (Şen 2014). The middle- and low-coverage grasslands accounted for 22.25% and 31.08% of the total catchment area, but the sediment yield amount in middle-coverage grassland was higher than that in low-coverage grassland in 2010. The results supported the fact that reasonable soil conservation practices could reduce soil erosion in sloping farmland and low-coverage grassland effectively (Lovell and Sullivan 2006) because the land management activities changed slope gradient and reduced flow accumulation (Melakua et al. 2018).

Hydrometeorological and landscape factors influencing sediment yield

Sediment yield in watersheds is heterogeneous in both time and space because it depends on many factors, such as climate, geology, soil type, geomorphology, land use, vegetation, and human activities (Verbist et al. 2010; Gourfi et al. 2018). First, the possible reasons for the irregular relationship between sediment yield and rainfall erosivity can be attributed to the actuality that the influencing factors of sediment yield process were more complex than soil erosion: (i) the upstream catchment of Ansai hydrological station is located in the semi-arid and arid region, the precipitation in this region is scarce and concentrated, the rainfall kinetic energy of few transient rainstorms may be easily lessened by vegetation interception, evaporation, and infiltration (Wu et al. 2018c), thus resulting in the reduction of erosive rainfall kinetic energy and sediment yield rate (Ai et al. 2017); (ii) there was a significant spatio-temporal difference for the distribution of erosive rainfall in this region (Wu et al. 2016d), the severe soil erosion may be always caused by a few pulsed heavy rainstorms or the medium intensity rainfalls with long duration, thus producing considerable sediment yield rate (Zheng et al. 2008).

Second, the soil conservation practices can effectively reduce runoff and sediment in the watersheds (Yan et al. 2015). The overall decreasing trends of sediment yield rate in the upstream catchment of Ansai hydrological station from 1981 to 2015 supported the findings that the large-scale “Grain for Green” project implemented in the late 1990s played a positive role in runoff and sediment reduction (Ai et al. 2013). Specifically, the decrease of sloping farmland (dry land) and

Table 4 Geospatial statistics of land-use type, land-use percentage, soil erosion grade, sediment yield, Minimum, Maximum and Mean sediment yield rate in the upstream catchment of Ansai hydrological station in 2010

Land-use type	Land-use percentage (%)	Soil erosion grade (E)	Sediment yield (10^4 t)	Sediment yield rate ($t \cdot km^{-2}$)		
				MIN	MAX	MEAN
Dry land in hilly area	35.76	Intensive < E < extreme	124.901	0.00	10,107.39	1073.84
Dry land in plain area	1.18	Micro < E < mild	5.282	0.00	8783.06	1376.20
Closed forest land	0.42	Mild < E < moderate	1.640	0.00	10,440.50	1200.66
Shrubland	1.62	Intensive < E < extreme	7.304	0.00	10,447.82	1386.17
Sparse forest land	1.08	Moderate < E < intensive	5.955	193.94	4428.09	1695.21
Other forest lands	6.37	intensive < E < extreme	23.975	0.00	12,162.58	1157.14
High coverage grassland	0.0113	Mild < E < moderate	0.069	0.00	12,881.51	1880.65
Middle-coverage grassland	22.25	Intensive < E < extreme	45.600	0.00	3157.94	630.10
Low-coverage grassland	31.08	Intensive < E < extreme	34.473	0.00	1169.38	341.01
Reservoir and pond	0.0211	Moderate < E < intensive	0.111	0.00	12,776.40	1611.36
Urban	0.0045	Micro < E < mild	0.020	165.35	3462.08	1351.73
Rural residential area	0.19	Mild < E < moderate	1.438	0.00	17,012.89	2326.11
Industrial and traffic construction land	0.0098	Micro < E < mild	0.025	0.00	9822.20	779.43

Chinese Soil Erosion Classification and Grading Standards (SL190-2007): water erosion (a) micro ($< 200, < 500, < 1000 t \cdot km^{-2} \cdot year^{-1}$) (b) mild ($200, 500, 1000-2500 t \cdot km^{-2} \cdot year^{-1}$) (c) moderate ($2500-5000 t \cdot km^{-2} \cdot year^{-1}$) (d) intensive ($5000-8000 t \cdot km^{-2} \cdot year^{-1}$) (e) extreme intensive ($8000-15,000 t \cdot km^{-2} \cdot year^{-1}$) (f) severe ($> 15,000 t \cdot km^{-2} \cdot year^{-1}$)

the increase of forestland/grassland can change land-use structures, which may cause an overall decrease in sediment yield rate from 1981 to 2015. More interestingly, it was not until 2007 that there was a sharp decrease in sediment yield rate and SDR. The delayed phenomenon of sediment reduction can be attributed to the cumulative effects of soil and water conservation practices since 1997 (López-Vicente et al. 2008), in other words, there is a practical lag period for the regulation of sediment delivery processes by the artificial vegetation construction because vegetation communities intercept sediment primarily by intercepting raindrops kinetic energy and reducing runoff erosivity (Zheng et al. 2007; Zhang et al. 2007) but vegetation needs a certain growth cycle before it can play an effective role in soil and water conservation (Qin et al. 2014).

Third, analysis of the relationships between sediment yield and rainfall-runoff characteristics can help to understand the factors and processes determining sediment responses (Nadal-Romero et al. 2008; Fang et al. 2011). In general, the annual variations of runoff and sediment yield are closely related to rainfall (Wei et al. 2015). The sharp increase of sediment yield in some extreme hydrological years can be partly explained by increased rainfall and larger peak flow events in the upstream catchment of Ansai hydrological station (Wu et al. 2019b). e.g., (i) The rainfall of 579.3 mm in 1988 was 1.12 times over the average annual rainfall of 519.5 mm, the runoff amount of $7446.82 \times 10^4 m^3$ was 1.53 times than the average annual runoff amount of $4870.27 \times 10^4 m^3$, the maximum peak flow was 1.83 times over the average value of $403 m^3 \cdot s^{-1}$, and the average sediment yield rate was 1.9 times

higher than the average value of $305.5 kg \cdot s^{-1}$. Actually, the transient rainstorm of only 50 min from 1:10 to 2:00 am in 1st September 1988 reached 17.5 mm, this rainstorm event was statistically characterized by a large covering area, short duration, and heavy intensity, which fully explained the reason for the abnormal increase of sediment yield rate in 1988. (ii) The rainfall of 548.1 mm in 1992 was 1.06 times over the average annual rainfall of 519.5 mm, the runoff amount of $9499 \times 10^4 m^3$ was 1.95 times over the average annual runoff amount of $4870.27 \times 10^4 m^3$, the maximum peak flow was 3.05 times over the average value of $403 m^3 \cdot s^{-1}$, and the average sediment yield rate was 4.27 times than the average value of $305.5 kg \cdot s^{-1}$. The results indirectly supported the findings by Qin et al. (2010) that annual runoff, sediment yield, and rainfall in large and medium watersheds were difficult to build direct interrelationships because the magnitude and timing of peak flow events were major determinants of the variability of sediment yield level (Ebabu et al. 2018).

Fourth, the annual change of the hydrometeorological parameters especially the increase of maximum peak flow was the main reason for the abrupt increase of sediment yield in the extreme hydrological years. However, the heavy rainstorm not only increased the sediment yield rate in the current year but also reduced the sediment yield rate in the following years, which is similar to the rules of sediment depletion during flood periods in some typical watersheds over the world (Gomez et al. 1997; Hudson 2003). Moreover, topography is also an important parameter affecting water erosion (Lee et al. 2012), as it is significantly related to the processes of sediment

transport under different underlying surfaces (Zheng et al. 2007). The study of sediment yield in the loess hilly and gully region has proven to be very complicated because of the numerous hydrometeorological and topographical parameters involved (Ebabu et al. 2018), the inconsistency or interrelation among these parameters (Ahmadi Mirghaed et al. 2018), and the lack of an appropriate method to quantify some of these parameters (Tetzlaff et al. 2013). This new overall understanding can act as an invaluable reference for decision-makers or planners who are interested in reducing soil loss, especially under heavy rainstorms.

Conclusions

Improved knowledge of the watershed-scale spatial and temporal variability of sediment yield is crucial to support the planning of conservation practices to control soil erosion, particularly in most severely eroded regions. (i) The dynamic multi-scale SDR algorithm supported by five long time series hydrometeorological data can be conveniently and legitimately applied in the spatio-temporal sediment yield predictions of the loess hilly and gully region, which provides extremely important clues for use in further developing a multi-scale ecohydrological decision-support system for watershed land-use planning, management, and policy. (ii) The annual dynamics of sediment yield depend on the inter-annual variation of SDR in a catchment. The overall decreasing trend of sediment yield rate especially after 2007 was closely related to the effective implementation and delayed effects of large-scale soil and water conservation practices. The high-risk regions of sediment yield mainly concentrated in the sloping farmlands locating at two sides of the river banks. The magnitude of SDR in the other two larger catchments with similar hydrometeorology, soil, topography, and land-use types varies greatly due to the scale effect of sediment transport process. (iii) Future sediment transport studies can focus on the development of physically-based SDR at different time and space scales, the quantification of SDR algorithm uncertainty, sensitivity analyses, and the integrated identification of microscopic mechanisms and macroscopic management for sediment or even pollutants, such as nutrients and chemicals. This new overall understanding creates opportunities for improving the prediction accuracy of sediment yield and designing the sustainable soil conservation planning in loess hilly and gully regions.

Funding information This study was financially supported by the National Natural Science Foundation of China (51679206), Tang Scholar (Z111021720), the Youth Science and Technology Nova Project in Shaanxi Province (2017KJXX-91), the Fundamental Research Funds for the Central Universities (2452016120, 2452015374), and the International Science and Technology Cooperation Funds (A213021603). This paper was also financially supported by the National Fund for Studying Abroad (CSC NO. 201706305014).

Compliance with ethical standards

Conflict of interest The authors declare that they have no competing interests.

References

- Ahmadi Mirghaed F, Souri B, Mohammadzadeh M, Salmanmahiny A, Mirkarimi SH (2018) Evaluation of the relationship between soil erosion and landscape metrics across Gorgan watershed in northern Iran. *Environ Monit Assess* 190(11):643
- Ai N, Wei TX, Zhu QK (2013) The effect of rainfall for runoff-erosion-sediment yield under the different vegetation types in Loess Plateau of Northern Shaanxi Province. *J Soil Water Conserv* 27(2):26–30
- Ai N, Wei TX, Zhu QK, Qiang FF, Ma H, Qin W (2017) Impacts of land disturbance and restoration on runoff production and sediment yield in the Chinese Loess Plateau. *Journal of Arid Land* 9(1):1–11
- Akbarzadeh A, Ghorbani-Dashtaki S, Naderi-Khorasgani M, Kerry R, Taghizadeh-Mehrjardi R (2016) Monitoring and assessment of soil erosion at micro-scale and macro-scale in forests affected by fire damage in northern Iran. *Environ Monit Assess* 188:699
- Alewell C, Borrelli P, Meusburger K, Panagos P (2019) Using the USLE: chances, challenges and limitations of soil erosion modelling. *Int Soil Water Conserv Res* 7(3):203–225
- Batista PVG, Silva MLN, Silva BPC, Curi N, Bueno IT, Acérbi Júnior FW, Davies J, Quinton J (2017) Modelling spatially distributed soil losses and sediment yield in the upper Grande river basin-Brazil. *Catena* 157:139–150
- Beskow S, Mello CR, Norton LD, Curi N, Viola MR, Avanzi JC (2009) Soil erosion prediction in the Grande River Basin, Brazil using distributed modeling. *Catena* 79(1):49–59
- Cai CF, Ding SW, Shi ZH, Huang L, Zhang GY (2000) Study of applying USLE and geographical information system IDRISI to predict soil erosion in small watershed. *J Soil Water Conserv* 14(2):19–24
- Cai QG, Fan HM (2004) On the factors and prediction models of SDR. *Prog Geogr* 23(5):1–9
- Cheng JM, Song T, Li Y (2012) Estimation of nitrogen and phosphorus loading of agricultural nonpoint sources along Nanxi Lake based on GIS. *Res Soil Water Conserv* 19(3):284–288
- de Vente J, Poesen J, Verstraeten G, Rompaey AV, Govers G (2008) Spatially distributed modelling of soil erosion and sediment yield at regional scales in Spain. *Glob Planet Chang* 60:393–415
- Diodato N, Bellocchi G (2010) Assessing and modelling changes in rainfall erosivity at different climate scales. *Earth Surf Process Landf* 34(7):969–980
- Dong YF, Wu YQ, Zhang TY, Yang W, Liu BY (2013) The sediment delivery ratio in a small catchment in the black soil region of Northeast China. *Int J Sediment Res* 28:111–117
- Ebabu K, Tsunekawa A, Haregeweyn N, Adgo E, Meshesha DT, Aklog D, Masunaga T, Tsubo M, Sultan D, Fenta AA, Yibeltal M (2018) Analyzing the variability of sediment yield: A case study from paired watersheds in the Upper Blue Nile basin, Ethiopia. *Geomorphology* 303:446–455
- Fang NF, Shi ZH, Li L, Jiang C (2011) Rainfall, runoff, and suspended sediment delivery relationships in a small agricultural watershed of the Three Gorges area, China. *Geomorphology* 135(1–2):158–166
- Foster GR, Wischmeier WH (1974) Evaluating irregular slopes for soil loss prediction. *Trans ASAE* 17:305–309
- Gao GJ (2012) Fractal features and scale transformation of watershed sediment transportation under LUCC. *J Anhui Agric Sci* 19: 10289–10293
- Golosov V, Collins AL, Tang Q, Zhang XB, Zhou P, He XB, Wen AB (2017) Sediment transfer at different spatial and temporal scales in

- the Sichuan hilly basin, China: synthesizing data from multiple approaches and preliminary interpretation in the context of climatic and anthropogenic drivers. *Sci Total Environ* 598:319–329
- Gomez B, Phillips JD, Magilligan FJ, James LA (1997) Floodplain sedimentation and sensitivity: summer 1993 flood, upper Mississippi River valley. *Earth Surf Process Landf* 22(10):923–936
- Gourfi A, Daoudi L, Shi Z (2018) The assessment of soil erosion risk, sediment yield and their controlling factors on a large scale: example of Morocco. *J Afr Earth Sci* 147:281–299
- Huang TCC, Lo KFA (2015) Effects of land use change on sediment and water yields in Yang Ming Shan National Park, Taiwan. *Environments* 2:32–42
- Hudson PF (2003) Event sequence and sediment exhaustion in the lower Panuco Basin, Mexico. *Catena* 52(1):57–76
- Jiang ZS, Zheng FL, Wu M (2008) China water erosion prediction model. Science Press, Beijing, pp 200–202
- Jiang ZS, Zheng FL, Wu M (2005) Prediction model of water erosion on hillslopes. *J Sediment Res* 4:1–6
- Kang HL, Wang WL, Xue ZD, Guo MM, Shi QH, Li JM, Guo JQ (2016) Erosion morphology and runoff generation and sediment yield on ephemeral gully in loess hilly region in field scouring experiment. *Trans Chin Soc Agric Eng* 32(20):161–170
- Keesstra SD, Temme AJAM, Schoorl JM, Visser SM (2014) Evaluating the hydrological component of the new catchment-scale sediment delivery model LAPSUS-D. *Geomorphology* 212:97–107
- Kinnell PIA (2016) Comparison between the USLE, the USLE-M and replicate plots to model rainfall erosion on bare fallow areas. *Catena* 145:39–46
- Kiniry JR, Williams JR, Srinivasan R (2000) Soil and water assessment tool user's manual. *Nat Clin Pract Rheumatol* 3(3):119–119
- Lee G, Yu W, Jung K (2012) Catchment-scale soil erosion and sediment yield simulation using a spatially distributed erosion model. *Environ Earth Sci* 70(1):33–47
- Lee SE, Kang SH (2013) Estimating the GIS-based soil loss and sediment delivery ratio to the sea for four major basins in South Korea. *Water Sci Technol* 68(1):124–133
- Li LY, Jiao JY, Chen Y (2009a) Research methods and results analysis of sediment delivery ratio. *Sci Soil Water Conserv* 7(6):113–122
- Li BB, Zheng FL, Long DC, Jiang ZS (2009b) Spatial distribution of soil erosion intensity in Zhifanggou small watershed based on GIS. *Sci Geogr Sin* 29(1):105–110
- Lin YP, Lin WC, Anthony J, Ding TS, Mihoub JB, Henle K, Schmeller DS (2018) Assessing uncertainty and performance of ensemble conservation planning strategies. *Landsc Urban Plan* 169:57–69
- Liu BY, Bi XG, Fu SH (2010) Beijing soil erosion equation. Science Press, Beijing, pp 52–67
- Liu BY, Nearing MA, Shi PJ, Jia ZW (2000) Slope length effects on soil loss for steep slopes. *Soil Sci Soc Am J* 64:1759–1763
- Liu JG, Cai QG, Zhang PC (2007) Temporal and spatial variations of sediment delivery ratio and its influencing factors in Chabagou Watershed. *Bull Soil Water Conserv* 27(5):6–10
- Long TY, Wu L, Li JC, He C (2012) Development of a dynamic adsorbed phosphorus pollution load model and its application to the Jialing River Basin, China. *Fresenius Environ Bull* 21(12):3920–3929
- López-Vicente M, Navas A, Machín J (2008) Identifying erosive periods by using rusle factors in mountain fields of the Central Spanish Pyrenees. *Hydrol Earth Syst Sci* 12(2):523–535
- Lovell ST, Sullivan WC (2006) Environmental benefits of conservation buffers in the United States: evidence, promise, and open questions. *Agric Ecosyst Environ* 112:249–260
- Lu H, Moran CJ, Sivapalan M (2005) A theoretical exploration of catchment-scale sediment delivery. *Water Resour Res* 41:1–15
- Ma CF, Ma JW, Buhe A (2001) Quantitative assessment of vegetation coverage factor in USLE model using remote sensing data. *Bull Soil Water Conserv* 21(4):6–9
- Ma LK, Liu GB, Li TH, Ni JR (2008) Fast evaluation of eco-environmental water requirement and water deficit in river basins II Application. *J Hydraul Eng* 39(11):1151–1159
- Markose VJ, Jayappa KS (2016) Soil loss estimation and prioritization of sub-watersheds of Kali River basin, Karnataka, India, using RUSLE and GIS. *Environ Monit Assess* 188:225
- Martinez-Casasnovas JA, Ramos MC, Ribes-Dasi M (2005) On-site effects of concentrated flow erosion in vineyards fields: some economics implications. *Catena* 60:129–146
- McCool DK, Brown LC, Foster GR, Mutchler CK, Meyer LD (1987) Revised slope steepness factor for the Universal Soil Loss Equation. *Trans ASAE* 30(5):1387–1396
- Melaku ND, Renschler CS, Flagler J, Bayud W, Klik A (2018) Integrated impact assessment of soil and water conservation structures on runoff and sediment yield through measurements and modeling in the Northern Ethiopian highlands. *Catena* 169:140–150
- Mhangara P, Kakembo V, Lim KJ (2012) Soil erosion risk assessment of the Keiskamma catchment, South Africa using GIS and remote sensing. *Environ Earth Sci* 65(7):2087–2102
- Miao YX, Fang XQ, Zhu Y, Wang K (2018) Hydrological elements variation feature analysis of the Yanhe River Basin over the last 50 years. *Geospatial Inf* 16(2):58–60
- Molla T, Sisheber B (2017) Estimating soil erosion risk and evaluating erosion control measures for soil conservation planning at Koga watershed in the highlands of Ethiopia. *Solid Earth* 8:1–23
- Nadal-Romero E, Regüés D, Latron J (2008) Relationships among rainfall, runoff, and suspended sediment in a small catchment with badlands. *Catena* 74:127–136
- Ndomba PM, Mtalio F, Killingtveit A (2009) Estimating gully erosion contribution to large catchment sediment yield rate in Tanzania. *Physics Chem Earth* 34(13–16):741–748
- Ondráčková L, Máčka Z (2019) Geomorphic (dis)connectivity in a middle-mountain context: human interventions in the landscape modify catchment-scale sediment cascades. *Area* 51:113–125
- Op de Hipt F, Diekkrüger B, Steup G, Yira Y, Hoffmann T, Rode M, Näschen K (2019) Modeling the effect of land use and climate change on water resources and soil erosion in a tropical West African catchment (Dano, Burkina Faso) using SHETRAN. *Sci Total Environ* 653:431–445
- Qin W, Cao WH, Zuo CQ, Wang ZY, Shan ZJ, Qin JT, Yan N, Zhang JF (2014) Runoff and sediment yield response to vegetation restoration in big and middle scale watershed of Loess Plateau. In: *The Ninth National Symposium on Basic Theory of Sediment*. China Water Power Press, Beijing, pp 720–727
- Qin W, Zhu QK, Liu GQ, Zhang Y (2010) Regulation effects of runoff and sediment of ecological conservation in the upper reaches of Beiluo River. *J Hydraul Eng* 41(11):1325–1332
- Renard KG, Foster GR, Weesies GA, McCool DK, & Yoder DC (1997). *Predicting soil erosion by water: a guide to conservation planning with the Revised Universal Soil Loss Equation (RUSLE)*. U.S. Department of Agriculture, Agriculture Handbook No. 703, 404 pp.
- Renard KG, Freimund JR (1994) Using monthly precipitation data to estimate the R-factor in the revised USLE. *J Hydrol* 157:287–306
- Sadeghi S, Mizuyama T, Miyata S, Gomi T, Kosugi K, Fukushima T, Mizugaki S, Onda Y (2008) Determinant factors of sediment graphs and rating loops in a reforested watershed. *J Hydrol* 356(3):271–282
- Sarma B, Sarma AK, Mahanta C, Singh VP (2015) Optimal ecological management practices for controlling sediment yield and peak discharge from hilly urban areas. *J Hydrol Eng* 20(10):04015005
- Şen Z (2014) Sediment yield estimation formulations for arid regions. *Arab J Geosci* 7(4):1627–1636
- Steegeen A, Govers G, Takken I, Nachtergaele J, Poesen J, Merckx R (2001) Factors controlling sediment and phosphorus export from two Belgian agricultural catchments. *J Environ Qual* 30:1249–1258
- Swamkar S, Malini A, Tripathi S, Sinha R (2018) Assessment of uncertainties in soil erosion and sediment yield estimates at ungauged

- basins: An application to the Garra River basin India. *Hydrol Earth Syst Sci* 22:2471–2485
- Taguas EV, Yuan Y, Bingner RL, Gómez JA (2012) Modeling the contribution of ephemeral gully erosion under different soil managements: a case study in an olive orchard microcatchment using the AnnAGNPS model. *Catena* 98:1–16
- Tang ZH, Cai QG, Zhang GY, Li ZW, Liu GH, Feng JL (2001) The soil erosion and sediment yield model in small watershed of Loess Hilly and gully region based on the water and sediment transport between land parcel. *J Sediment Res* 10:48–53
- Temme AJAM, Claessens L, Veldkamp A, Schoorl JM (2011) Evaluating choices in multi-process landscape evolution models. *Geomorphology* 125:271–281
- Tetzlaff B, Friedrich K, Vorderbrügge T, Vereecken H, Wendland F (2013) Distributed modelling of mean annual soil erosion and sediment delivery rates to surface waters. *Catena* 102:13–20
- Tetzlaff B, Vereecken H, Kunkel R, Wendland F (2009) Modelling phosphorus inputs from agricultural sources and urban areas in river basins. *Environ Geol* 57:183–193
- Toy TJ, Foster GR, Renard KG (2002) *Soil erosion: processes, prediction, measurement, and control*. John Wiley & Sons Inc, New York
- Verbist B, Poesen J, van Noordwijk M, Suprayogo D, Agus F, Deckers J (2010) Factors affecting soil loss at plot scale and sediment yield at catchment scale in a tropical volcanic agroforestry landscape. *Catena* 80(1):34–46
- Wang F, Mu XM, Jiao JY, Li R (2008b) Impact of human activities on runoff and sediment change of Yanhe River based on the periods divided by sediment concentration. *J Sediment Res* 4:8–13
- Wang L, Shao MA, Wang QJ, Gale W (2006) Historical changes in the environment of the Chinese loess plateau. *Environ Sci Pol* 9:675–684
- Wang LL, Yao WY, Liu LY, Li M (2008a) Research progress on sediment transport ratio in China. *Yellow River* 30(9):36–37 45
- Wang XY, Tian JL, & Yang MY (2003). The application of tracing method in the sediment study. *J Sediment Res*, (1), 18–23
- Wang XY, Wang XF, Wang QP, Wang ZG, Cai XG (2004) Loss of nonpoint source pollutants from Shixia small watershed, Miyun Reservoir, Beijing. *Sci Geogr Sin* 24(2):227–231
- Wang Y, Feng Q (2017) Characteristics of runoff and sediment transport during 1960-2010 and its response to Grain for Green Project in Yanhe River. *Sci Soil Water Conserv* 15(1):1–7
- Wang ZJ, Ma LM, Jiao JY (2013) Sediment delivery ratio in different spatial scale watershed in Loess Hill-gully region. *Bull Soil Water Conserv* 33(6):1–8
- Watling JI, Brandt LA, Bucklin DN, Fujisaki I, Mazzotti FJ, Romañach SS, Speroterra C (2015) Performance metrics and variance partitioning reveal sources of uncertainty in species distribution models. *Ecol Model* 309:48–59
- Wei W, Chen LD, Zhang HD, Chen J (2015) Effect of rainfall variation and landscape change on runoff and sediment yield from a loess hilly catchment in China. *Environ Earth Sci* 73:1005–1016
- Wischmeier WH, & Smith DD (1965). Predicting rainfall-erosion losses from cropland east of the Rocky Mountains: guide for selection of practices for soil and water conservation. Agricultural Research Service, U.S. Department of Agriculture, Agriculture Handbook, No. 282
- Wischmeier WH, & Smith DD (1978). Predicting rainfall erosion losses—a guide to conservation planning. Agricultural Research Service, U.S. Department of Agriculture, Agriculture Handbook, No. 537
- Woznicki SA, Pouyan Nejadhashemi A (2013) Spatial and temporal variabilities of sediment delivery ratio. *Water Resour Manag* 27:2483–2499
- Wu A, Li TH, & Han P (2014). Relationship between sediment delivery ratio and basin area in Yellow River Basin. *J Sediment Res*, (1), 61–67
- Wu L, He Y, Ma XY (2020) Can soil conservation practices reshape the relationship between sediment yield and slope gradient? *Ecol Eng* 142:105630
- Wu L, Liu X, Ma XY (2016a) Application of a modified distributed-dynamic erosion and sediment yield model in a typical watershed of hilly and gully region, Chinese Loess Plateau. *Solid Earth* 7(6): 1577–1590
- Wu L, Liu X, Ma XY (2016b) Spatio-temporal variation of erosion-type non-point source pollution in a small watershed of hilly and gully region, Chinese Loess Plateau. *Environ Sci Pollut Res* 23:10957–10967
- Wu L, Liu X, Ma XY (2016c) Tracking soil erosion changes in an easily-eroded watershed of the Chinese loess plateau. *Pol J Environ Stud* 25(1):332–344
- Wu L, Liu X, Ma XY (2016d) Spatiotemporal distribution of rainfall erosivity in the Yanhe River watershed of hilly and gully region, Chinese Loess Plateau. *Environ Earth Sci* 75:315
- Wu L, Qi T, Zhang J (2017) Spatiotemporal variations of adsorbed non-point source nitrogen pollution in a highly erodible Loess Plateau watershed. *Pol J Environ Stud* 26(3):1343–1352
- Wu L, Liu X, Ma XY (2018a) Research progress on the watershed sediment delivery ratio. *Int J Environ Stud* 75(4):565–579
- Wu L, Yao WW, Ma XY (2018b) Using the comprehensive governance degree to calibrate a piecewise sediment delivery ratio algorithm for dynamic sediment predictions: A case study in an ecological restoration watershed of Northwest China. *J Hydrol* 564:888–899
- Wu L, Jiang J, Li GX, Ma XY (2018c) Characteristics of pulsed runoff-erosion events under typical rainstorms in a small watershed on the Loess Plateau of China. *Sci Rep* 8:3672
- Wu L, Li XP, Ma XY (2019a) Particulate nutrient loss from drylands to grasslands/forestlands in a large-scale highly erodible watershed. *Ecol Indic* 107:105673
- Wu L, Li GX, Jiang J, Ma XY (2019b) Using vegetation correction coefficient to modify a dynamic particulate nutrient loss model for monthly nitrogen and phosphorus load predictions: a case study in a small loess hilly watershed. *Environ Sci Pollut Res*. <https://doi.org/10.1007/s11356-019-06564-2>
- Xie HX (2008) Study on the spatio-temporal change of soil loss and on the assessment of impacts on environment of soil and water conservation in Yanhe Basin. Doctoral Dissertation of Shaanxi Normal University, Xi'an, pp 47–59
- Xie WC, Li TH (2012) Research comment on watershed sediment delivery ratio. *Acta Sci Nat Univ Pekin* 48(4):685–694
- Yan QH, Lei TW, Yuan CP, Lei QX, Yang XS, Zhang ML, Su GX, An LP (2015) Effects of watershed management practices on the relationships among rainfall, runoff, and sediment delivery in the hilly-gully region of the loess plateau in China. *Geomorphology* 228:735–745
- Yavuz M, Tufekcioglu M (2019) Estimating surface soil losses in the mountainous semi-arid watershed using RUSLE and geospatial technologies. *Fresenius Environ Bull* 28(4):2589–2598
- Yu XX, Zhang ML, Xin ZB (2011) *Eco-hydrological response to multi-scale watershed environmental evolution in the Loess Plateau*. Science Press, Beijing, pp 151–158
- Zhang JR, Yue DP, Da X, Cheng JW, He YZ (2017) Quantitative analysis on impacts of climate change and human activities on sediment yield in the Yanhe River Basin. *Shandong Agric Sci* 49(3):106–112
- Zhang L, Miao LP, Wen ZM (2005) Estimating the effect of vegetation and precipitation on runoff and sediment using the MMF model: a case study in the Yanhe River Basin. *J Natl Resour* 30(3):446–458
- Zhang KL, Peng WY, Yang HL (2007) Soil erodibility and its estimation for agricultural soil in China. *Acta Pedol Sin* 44(1):7–13
- Zhang XM, Cao WH, Zhou LJ (2014) Progress review and discussion on sediment delivery ratio and its dependence on scale. *Acta Ecol Sin* 34(24):7475–7485
- Zhang XY, Li QS (2018) Effects of land use types on soil erosion and soil nutrient losses in purple soil. *Res Soil Water Conserv* 25(5):12–17

- Zheng FL, Xiao PQ (2010) Evolution process of gully erosion and sediment yield in the Loess Plateau. Science Press, Beijing
- Zheng MG, Cai QG, Chen H (2007) Effect of vegetation on runoff-sediment relationship at different spatial scale levels in gullied-hilly area of the Loess Plateau, China. *Acta Ecol Sin* 27(9):3572–3581
- Zheng MG, Cai QG, Cheng QJ (2008) Modelling the runoff-sediment yield relationship using a proportional function in hilly areas of the Loess Plateau, North China. *Geomorphology* 93(3–4):288–301
- Zhu HF, Kang MY, Zhao WW, Guo WW (2007) Effects of soil and water conservation measures on erosion, sediment delivery and deposition in the Yanhe River Basin. *Res Soil Water Conserv* 14(4):1–4
- Zhu TX (2012) Gully and tunnel erosion in the hilly Loess Plateau region, China. *Geomorphology* 153–154:144–155

Publisher's note Springer Nature remains neutral with regard to jurisdictional claims in published maps and institutional affiliations.